Radio signals from electron beams in Terrestrial Gamma-ray Flashes

Valerie Connaughton,[1,2] Michael S. Briggs,[1,2] Shaolin Xiong,[1] Joseph R. Dwyer,[3] Michael L. Hutchins,[4] J. Eric Grove,[5] Alexandre Chekhtman,[6] Dave Tierney,[7] Gerard Fitzpatrick,[7] Suzanne Foley,[7] Shelia McBreen,[7] P. N. Bhat,[1] Vandiver L. Chaplin,[1] Eric Cramer,[3] Gerald J. Fishman,[8] Robert H. Holzworth,[4] Melissa Gibby,[8] Andreas von Kienlin,[9] Charles A. Meegan,[10] William S. Paciesas,[10] Robert D. Preece,[1,2] and Colleen Wilson-Hodge.[11]

P. N. Bhat, M. S. Briggs, V. Chaplin, V. Connaughton, R. D. Preece, and S. Xiong, CSPAR, 320 Sparkman Drive, Huntsville, AL, 35805, USA. (valerie@nasa.gov).

J. R. Dwyer and E. Cramer, Physics and Space Sciences, Florida Institute of Technology, Melbourne, FL 32901, USA. (jdwyer@fit.edu)

R. H. Holzworth and M. L. Hutchins, Earth and Space Sciences, University of Washington, Seattle, WA 98195, USA. (bobholz@ess.washington.edu)

G. Fitzpatrick, Suzanne Foley, S. McBreen and D. Tierney, School of Physics, University College Dublin, Belfield, Dublin 4, Ireland. (sheila.mcbreen@ucd.ie)

A. Chekhtman and J. E. Grove, Space Science Division, U. S. Naval Research Laboratory, Washington, D.C., 20375, USA. (eric.grove@nrl.navy.mil)

G. J. Fishman and M. Gibby, Jacobs Engineering Group Inc., 1500 Perimeter Parkway, Huntsville, AL 35806, USA. (jerry.fishman@nasa.gov)

A. von Kienlin, Max-Planck Institut für extraterrestrische Physik, D-85741 Garching, Germany. (azk@mpe.mpg.de)

C. A. Meegan and W. S. Paciesas, USRA, 320 Sparkman Drive, Huntsville, AL, 35805, USA. (chip.meegan@nasa.gov).

C. Wilson-Hodge, Space Science Office, VP62, NASA Marshall Space Flight Center, Huntsville, AL, 35812, USA. (Colleen.Wilson@nasa.gov)

[1]CSPAR, University of Alabama in Huntsville, Huntsville, AL, 35899, USA

[2]Dept. of Physics, University of Alabama in Huntsville, Huntsville, AL, 35899, USA

[3]Physics and Space Sciences, Florida Institute of Technology, Melbourne, FL 32901, USA

[4]Earth and Space Sciences, University of Washington, Seattle, WA 98195, USA

[5]Space Science Division, U. S. Naval Research Laboratory, Washington, D.C., 20375, USA

[6]George Mason University, Fairfax, VA, 22030, USA

[7]University College Dublin, Belfield, Dublin 4, Ireland

[8]Jacobs Engineering Group Inc., Huntsville, AL 35806, USA.

[9]Max-Planck Institut für extraterrestrische Physik, D-85741 Garching, Germany

[10]Universities Space Research Association, Huntsville, AL, 35803, USA

Abstract. We show that the rate of association between Terrestrial Gamma-ray Flashes (TGFs) observed by the Fermi Gamma-ray Burst Monitor (GBM) and Very-Low Frequency (VLF) discharges detected by the World Wide Lightning Location Network (WWLLN) depends strongly on the duration of the TGF, with the shortest TGFs having associated WWLLN events over 50% of the time, and the longest TGFs showing a less than 10% match rate. This correlation is stronger if one excludes the WWLLN discharges that are not simultaneous (within 200 μs) with the TGF. We infer that the simultaneous VLF discharges are from the relativistic electron avalanches that are responsible for the flash of gamma rays and the non-simultaneous VLF discharges are from related Intra-Cloud lightning strokes. The distributions of far-field radiated VLF stroke energy measured by WWLLN for the simultaneous and non-simultaneous discharges support the hypothesis of two discrete populations of VLF signals associated with TGFs, with the simultaneous discharges among the strongest measured by WWLLN.

[11]Space Science Office, NASA Marshall

Space Flight Center, Huntsville, AL, 35812,

USA

1. Introduction

Terrestrial Gamma-ray Flashes (TGFs) are brief bursts of high-energy radiation discovered by the Burst And Transient Source Experiment (BATSE) [*Fishman et al.*, 1994], and detected since then by several high-energy satellite detectors: the Reuven Ramati High Energy Solar Spectroscopic Imager (RHESSI) [*Smith et al.*, 2005; *Grefenstette et al.*, 2009; *Gjesteland et al.*, 2012], the Astrorivelatore Gamma a Immagini Leggero (AGILE) [*Marisaldi et al.*, 2010a; *Fuschino et al.*, 2009; *Marisaldi et al.*, 2010b], and most recently by the Gamma-ray Burst Monitor (GBM) on-board the Fermi Satellite [*Briggs et al.*, 2010; *Fishman et al.*, 2011]. Their connection to lightning was suspected since their discovery as the first detections occurred in satellites overflying regions with active thunderstorms. TGFs are believed to originate in the large-scale electric fields near the tops of thunderclouds and likely involve the acceleration and multiplication of electrons emitting bremsstrahlung radiation and eventually discharging the field. Ground-based networks detecting the Ultra-Low or Very-Low Frequency (ULF or VLF) radio signals from electric field discharges found in coincidence with TGFs have been used to locate the sources of TGFs to a small region within the larger footprint of the satellite over the Earth. Correlations in time between electric field discharges and TGFs suggested a temporal separation of no more than a few milliseconds [*Inan et al.*, 1996; *Cummer et al.*, 2005; *Stanley et al.*, 2006; *Inan et al.*, 2006; *Lay*, 2008; *Cohen et al.*, 2006, 2010] with more precise relative timing hindered by a ~ 2 ms uncertainty in RHESSI timing and limitations of the BATSE-era radio networks. Using the timing accuracy of Fermi GBM and the World Wide Lightning Location Network (WWLLN) [*Rodger et al.*, 2009], *Connaughton*

et al. [2010] showed that 15 of the first 50 TGFs that triggered GBM were associated with a WWLLN-measured discharge, and that most of these discharges occurred near the time of a TGF pulse peak. Of these associations within 5 ms of a TGF peak, 13 occured within tens of μs of the peak, with one WWLLN discharge each between 1 and 5 ms either side of the peak. The sample of GBM TGFs has greatly increased in size from the 50 events reported in *Connaughton et al.* [2010]. In addition to 130 additional triggered TGFs, a new data taking mode has been implemented whereby individual time-tagged photons are downlinked when Fermi passes over regions of expected thunderstorm activity. These regions are predefined and modified seasonally according to weather patterns. TGFs can then be found on the ground in an offline search, rather than having to trigger on-board in a 16 ms window wherein only the brightest TGFs are visible above threshold [*Briggs et al.*, 2012]. We explore here the correlation between WWLLN-measured discharges and a population of 601 TGF pulses that were detected between 08 August 2008 and 30 August 2011, of which 180 were triggered TGFs (192 pulses) and 409 were uncovered using the offline search. In addition to the 384 TGFs from the offline search [*Briggs et al.*, 2012], of which three had two peaks that are counted separately, 22 TGFs were found outside the time period or geographic region reported in that work, mostly in the time-tagged event data surrounding triggered TGFs.

2. Results

Guided by prior TGF-radio correlation results, we defined three search radii: (i) 300 km, identified in *Connaughton et al.* [2010] as the horizon for all the WWLLN discharges associated with 15 triggered TGFs, (ii) 600 km radius as used in *Hazelton et al.* [2009] and *Cohen et al.* [2010] to contain associations between RHESSI-detected TGFs and radio

signals, and (iii) 1000 km, as a more speculative choice to explore the possibility that, with the offline search, GBM might be sensitive to weaker events from a larger distance. Likewise, the 5 ms window defining an association with radio signals in both RHESSI and GBM searches so far was retained, but two new windows (10 and 20 ms) were introduced because the small number of TGFs found in *Connaughton et al.* [2010] that were associated but not simultaneous with the TGF (i.e., not within $\pm 40\,\mu$s) did not delineate a clear time boundary either side of the TGF for determining statistically significant associations. We calculate the probability of each association being a coincidence by finding the number of matches in the WWLLN data of 1000 proxy TGF times at 1 s intervals within $\pm$500 s of the TGF trigger time [*Connaughton et al.*, 2010]. We treat each time window and horizon as a separate control sample for the purpose of determining the chance probability of each match given the clustering of WWLLN events on the relevant timescale and geographical region. A chance probability of more than 1% - 10 matches in the control sample - was used to dismiss an association as a possible coincidence. In the sample of 601 TGFs, 198 produced WWLLN matches in one or more of the windows described above. Twelve of these were rejected using an unacceptably high match rate in the control sample, of which three were within the 5 ms window, and six beyond the 10 ms window. Of the 186 significant matches, 182 were found within the 5 ms coincidence window. Three of the remaining four were found in the 5 - 10 ms window, with only one in the 10 - 20 ms window, suggesting that expanding the time window does not reveal many TGF/WWLLN associations, and those that are found in the expanded window have a high probability of occurring by chance.

Because the TGFs uncovered in the offline GBM search are weaker and have limited counting statistics, the pulse-fitting technique described in *Briggs et al.* [2010] and employed in *Connaughton et al.* [2010] to establish the TGF peak time becomes difficult. Instead, we take the center of the T_{50} period, i.e., the period during which 50% of the total TGF fluence is observed, starting from the 25% fluence level time [*Fishman et al.*, 2011]. The peak is not located as precisely using this method as with the pulse-fitting algorithm, and we reestablish our definition of GBM-WWLLN simultaneity by examining the temporal offsets between the WWLLN discharge times of group arrival and the TGF T_{50} center times, corrected for light travel time to Fermi, shown in Figure 1. The $\pm 40\,\mu$s envelope for simultaneity established in *Connaughton et al.* [2010] is expanded to $\pm 200\,\mu$s. This $400\,\mu$s interval centered on the mid-point of the T_{50} is well-matched to the typical duration of a TGF, which we characterize by T_{90}, the 5% to 95% fluence accumulation period [*Briggs et al.*, 2012]. Although the T_{50} interval contains only 50% of the TGF fluence, we adopt it here as a more robust measure of duration compared to T_{90} because it is less susceptible to uncertainties caused by low count rates and background counts in the tail of the TGF. Using these definitions, 154 of the 186 WWLLN discharges are simultaneous with the gamma-ray peak of the TGF. No WWLLN discharges simultaneous with the TGF had enough matches in the control samples to cause their rejection as real associations.

In contrast to the expanded time windows, the expanded search radii revealed many WWLLN matches, particularly among the TGFs found offline, but even some of the triggered TGFs occurred beyond the 300 km horizon established in *Connaughton et al.* [2010]. The most distant association that passed the control sample test was 954 km

from the Fermi nadir. The spacecraft was flying over Madagascar, and examination of the WWLLN lightning map during the 20 minutes surrounding the TGF reveals storm systems that are closer to the spacecraft nadir and more credible as the source of the TGF. The angular offset distribution of TGFs is shown in Figure 7 of *Briggs et al.* [2012] to decline beyond 300 km and tail off smoothly by 800 km. We cannot dismiss the more distant match using our established rejection criteria, but the fact that the second farthest WWLLN discharge associated with a TGF is 200 km closer to the nadir suggests that this 954 km match may be a false positive. Based on this reasoning, we consider the maximum horizon for a WWLLN discharge to be a credible association with a GBM TGF to be around 800 km. An all-sky search for matches revealed eight beyond the 1000 km limit of this analysis, all of which produced unacceptable chance coincidences in the control samples, and all but one of them outside the 5 ms time window. This suggests that one needs to worry about false associations using the WWLLN data when searching at large source distance and temporal offsets in the expanded time windows but that the results of our search within the narrow time window and up to eight hundred km search radius are reliable.

The match rate in the population of TGFs that triggered GBM (26%) is lower than in the offline search sample (33%), meaning that the TGFs that show fewer counts in the GBM detectors are more likely to be associated with a discharge measured by WWLLN, a result that seems puzzling if one considers that for a given intrinsic TGF intensity the number of counts detected by GBM depends only on the TGF-Fermi geometry. The measured intensity is inversely proportional to the square of the source distance from Fermi for a given angular offset, and is strongly influenced by atmospheric attenuation. For

TGFs viewed at larger angular offsets, the measured flux is lower when Fermi measures scattered flux outside the direct beam [*Østgaard et al.*, 2008; *Hazelton et al.*, 2009; *Collier et al.*, 2011; *Gjesteland et al.*, 2011]. These factors should not affect the likelihood of the associated discharge being measured by WWLLN. A Kolmogorov-Smirnov (KS) test of the T_{50} count fluence distributions of the 186 and 408 TGFs with and without associated WWLLN discharges gives a probability of 0.09 that they are drawn from the same population, with this probability decreasing to 0.07 if one considers only the 154 TGFs with simultaneous WWLLN discharges. This is suggestive of a correlation between TGF fluence and the detection of an associated discharge by WWLLN, a link that was also noted by *Collier et al.* [2011] and *Gjesteland et al.* [2012] in an analysis of RHESSI TGFs and WWLLN events. While the statistical significance of the match rate versus gamma-ray counts is modest in the GBM sample, the prior detection of this correlation in an independent sample indicates that it is not due to chance. We find, however, a more striking correlation when instead of comparing the fluence distributions of the samples of TGFs with and without associated WWLLN discharges, we compare the duration distributions of these two samples. This comparison yields a KS probability of 10^{-12} that the T_{50} distributions of the TGFs with and without WWLLN associations are drawn from the same population, decreasing to 10^{-16} if we restrict the sample with WWLLN matches to the 154 TGFs with simultaneous WWLLN discharges. These T_{50} distributions are displayed in Figure 2 (top panel), which also illustrates that the rate of association between TGFs and WWLLN discharges increases steadily with decreasing TGF duration (lower panel). A Spearman's rank-order correlation of -0.97 is found for the WWLLN match-rate fraction as a function of T_{50}, corresponding to a probability of 2×10^{-5} that

this correlation occurred by chance. This relation is even tighter if we exclude the 32 TGFs for which the WWLLN discharge is not simultaneous with the TGF, indicating a near-perfect anti-correlation between the durations of TGFs and the detection rate of associated simultaneous discharges by WWLLN.

3. Discussion

We have established that the TGFs detected using GBM show an approximately 30% rate of associations with discharges measured by WWLLN, down to the weakest TGFs detected so far, and that this association rate varies according to the duration of the TGF. Using the National Lightning Detection Network (NLDN) as ground truth, the efficiency for lightning detection of WWLLN over the US was estimated to be around 10% in 2008 for Cloud-to-Ground lightning when GBM began operations [*Abarca et al.*, 2010] with lower efficiencies outside the US and Caribbean [*Hutchins et al.*, 2012a]. This efficiency has improved with the addition of new receiving stations and the development of more sophisticated signal processing algorithms [*Rodger et al.*, 2009], but it is imperfect, limited by the size of the discharge that is measured at multiple stations and triangulated at the time of its estimated peak power, and varies according to changing ionospheric conditions (day-night effects), differences in VLF propagation over land, oceans, and ice, and the presence of local lightning activity, which raises the detection threshold for more distant strokes [*Hutchins et al.*, 2012a]. According to the detection efficiency calculations of *Abarca et al.* [2010], our association rate of 30% suggests that if discharges seen in association with TGFs are attributable to lightning, then they have unusually high currents, and that the shorter TGFs are associated with the strongest discharges measured by WWLLN. Using the match rates from Figure 2 one can use the WWLLN stroke detection efficiency as a

function of peak current presented in Figure 3 of *Abarca et al.* [2010] to infer an average peak current for each T_{50} time bin. TGFs longer than 210 μs are associated with currents below 10 kA, those lasting from 90 to 210 μs range from 80 kA to 35 kA, and the shortest TGFs with a greater than 50% match rate are associated with currents above 150 kA. This suggests a puzzling dependence on TGF duration of the current from the associated lightning discharge.

If instead of lightning, WWLLN is detecting the TGF itself [*Cummer et al.*, 2011; *Dwyer*, 2012], then a relationship between the characteristics of the TGF and its detectability by WWLLN is more natural. Let us consider the electrical currents and the resulting radio frequency emissions that are generated by the runaway electron avalanches that compose the TGF. Here, we do not include any electrical currents that might be directly made by the lightning processes [*Carlson et al.*, 2010]. As the runaway electrons propagate, they ionize the air, creating low-energy (few eV) electrons and ions that drift in the electric field. Most of the electrical current generated by the runaway electron avalanches comes from the drifting low-energy electrons. Because these low-energy electrons quickly attach to oxygen atoms, usually on a time scale less than a few μs, the electrical current generated by the TGF will closely follow the time-structure of the TGF gamma rays at the source. At spacecraft altitudes the duration of the TGF may be increased due to Compton scattering in the atmosphere [*Østgaard et al.*, 2008; *Grefenstette et al.*, 2008; *Gjesteland et al.*, 2010]. However, the higher energy photons ($>$ 1 MeV) will most closely match the original duration of the TGF at the source, since these photons will have undergone the least Compton scattering.

Following *Dwyer* [2012] we consider a rate of runaway electrons [number per sec] that follows a Gaussian distribution in time with RMS, σ. For a Gaussian distribution, $\sigma = 0.74T_{50}$. The current moment as a function of time is then

$$I_{mom} = \frac{e\alpha\tau_a\mu_e E N_{re}\Delta z}{\sqrt{2\pi}0.74T_{50}}\exp\left(\frac{-\mathrm{t}^2}{2(0.74\mathrm{T}_{50})^2}\right) \quad (1)$$

where e is the charge of the electron; α is the ionization per unit length per runaway electron; μ_e is the mobility of the low-energy electrons, τ_a their attachment time; E is the electric field strength; N_{re} is the total number of runaway electrons; and Δz is the vertical distance over which the runaway electrons travel [*Dwyer*, 2012]. From RHESSI observations, at an altitude of 13 km, the combination $N_{re}\Delta z = 1.5 \times 10^{20}$ m [*Dwyer and Smith*, 2005; *Dwyer*, 2012]. At 13 km, $\tau_a = 1.3 \times 10^{-6}$ s, $\mu_e = 0.4\,m^2/Vs$ [*Morrow and Lowke*, 1997; *Liu and Pasko*, 2004] and $\alpha = 1,900\,m^{-1}$ (scaled from a sea-level value of $8,350\,m^{-1}$) [*Dwyer and Babich*, 2011]. Finally, most of the runaway electrons are produced at the end of the avalanche region where $E = 2.84 \times 10^5\,V/m \times n = 6.4 \times 10^4\,V/m$, where n is the density of air relative to sea level.

As can be seen from Eq. 1, for the same number of runaway electrons and hence the same number of gamma rays emitted at the source, a shorter TGF produces a larger peak current moment. Furthermore, a shorter TGF emits more radio frequency (RF) energy at higher frequencies, which is important when considering the frequency threshold of WWLLN (> 6 kHz).

At large horizontal distances, the radiation electric field emitted by the current moment, I, in Eq. 1 is given by

$$E_{rad} = \frac{\sin\theta}{4\pi\varepsilon_0 c^2 R}\frac{\partial I}{\partial t} \tag{2}$$

where all the symbols have their usual meaning [*Uman*, 2001]. Inserting Eq. 1 into Eq. 2 and taking the Fourier transform gives

$$E(\omega) = -i\omega\frac{e\alpha\tau_a\mu_e E N_{re}\Delta z\sin\theta}{\sqrt{2\pi}4\pi\varepsilon_0 c^2 R}\exp\left(\frac{-\omega^2(0.74\mathrm{T}_{50})^2}{2}\right) \tag{3}$$

where ω is the angular frequency. The spectral energy density (energy radiated per unit frequency) is proportional to the square of Eq. 3.

WWLLN was optimized for measuring lightning, which has peak spectral energy density around 10 kHz. Its detectors record the RF signal from 1 to 24 kHz, with data between 6 and 18 kHz contributing to the nominal analysis. *Jacobson et al.* [2006] found a significant fraction of intra-cloud (IC) lightning discharges correlated with very short duration ($\sim 20\,\mu$s) Narrow Bipolar Events detected by the Los Alamos Sferic Array, suggesting a high WWLLN efficiency for detecting powerful short events. From Eq. 3, the TGF will also produce an RF signal with a peak spectral energy density at 10 kHz, similar to lightning, when $T_{50} = 21.5\,\mu$s. In this case, the peak current moment (Eq. 1) is 40 kA-km. If we assume that $\Delta z \sim 1$ km, then the peak current in this case is 40 kA, a large value, comparable to lightning. Therefore, it is expected that the WWLLN would efficiently detect such short TGFs.

On the other hand, as can be seen in Eq. 3, the energy radiated into the WWLLN detection band falls very quickly as T_{50} increases. For example, for $T_{50} = 150\,\mu$s, the energy radiated into the 6 - 18 kHz band is 6×10^7 times smaller than the energy radiated

into that band when $T_{50} = 50\,\mu$s [*Hutchins et al.*, 2012a]. From Eq. 1 we would expect the detection efficiency to decrease greatly with increased T_{50} values, but the observed decrease (Figure 2) is much more gradual than expected from Eq. 3.

We consider several explanations to explain the WWLLN efficiency for longer TGFs being higher than expected in our simple model. First, there could be additional lightning currents during many TGFs that, when added to the currents from the TGF itself, combine to put the event over the WWLLN detection threshold for longer TGFs. Second, a TGF arising deeper in the atmosphere than the 13 km assumed in Eq 1 will yield more electrons and a higher current, since more runaway electrons are needed to produce the same fluence of gamma rays exiting the atmosphere. Third, our characterization of TGF duration is subject to observational and instrumental effects. Longer TGFs may contain substructure (shorter current pulses) that efficiently radiate in the WWLLN frequency band. *Briggs et al.* [2010] show that in addition to multi-pulse TGFs that we consider here on a per-pulse basis, some TGFs are likely a superposition of shorter pulses (see also *Celestin and Pasko* [2012]), and that some pulses are Gaussian and others are better fit using a log normal function that can have a very fast rise time, as short as $7\,\mu$s. In general, our assumption regarding the Gaussian shape of a TGF gives a rather pessimistic prediction for WWLLN detection, and a sharper rise or decay will yield more energy at higher frequencies. For some TGFs, Compton scattering may make the duration of the gamma-ray flash measured by GBM significantly longer than the duration of the electron avalanche. Some of the long TGFs, then, might be efficiently detected by WWLLN, while others might be intrinsically long and do not produce enough RF energy in the WWLLN band to be detected. The T_{50} values in Figure 2 are measured over the entire energy

range seen by GBM (8 keV - 40 MeV). If we restrict the T_{50} calculation to energies above 300 keV, we can see from Figure 3 that the number of shorter TGFs with associated WWLLN discharges is higher and the rate of longer TGFs with WWLLN matches lower, an effect that is not seen in the TGF population without WWLLN matches. Owing to poor statistics, the T_{50} measurement becomes difficult when the energy range is further restricted, but the fact that longer events with WWLLN matches appear shorter at higher energies supports the hypothesis that their duration is lengthened by Compton scattering on the way to Fermi. A final instrumental effect concerns the deadtime suffered in the GBM detectors. One effect of deadtime is to underestimate the intensity at the peak of the TGF, thus artificially lengthening the T_{50} estimate. The effect of deadtime can also explain the higher match rate of the population of TGFs from the offline search if we consider a population of TGFs, all with about the same fluence of gamma rays at the source, but with a distribution of durations. In this population, the ones that are most likely to have a match are the very short ones (keeping in mind that they may appear longer in GBM due to Compton scattering and deadtime). Because of dead time, the number of photons detected by GBM should always be less for shorter TGFs. Therefore when the fluence (total numbers of counts) threshold of a GBM TGF sample is lowered, the proportion of short TGFs will increase, causing the WWLLN match rate of the sample to increase. Both effects are seen in the offline search sample of *Briggs et al.* [2012], and this reasoning can also explain the result from *Collier et al.* [2011] and *Gjesteland et al.* [2012] that the weaker RHESSI TGFs have a higher WWLLN association rate. It is not the weakness of the TGF that makes it more likely to have a WWLLN association but its shortness: a short TGF is more likely to have fewer counts than a longer TGF.

The combination of instrumental effects (deadtime), source behavior (Compton scattering, overlapping pulses, non-Gaussian shapes, fast risetimes), and model assumptions (contributions to current from lightning, source height) complicates the relationship between WWLLN detection rate and TGF duration, although it is qualitatively as one would expect if the TGF is responsible for the radio signal. Given the close relationship expected between the RF signal and the gamma-ray time profile, only the simultaneous associations can be attributed to the TGF itself. The WWLLN associations that are not simultaneous (greater than $\pm 200\,\mu$s from the TGF peak) but still significantly temporally and spatially coincident with the TGF could then be discharges from regular IC lightning activity that is also believed to be associated with TGFs [*Stanley et al.*, 2006; *Lu et al.*, 2010]. The time boundary between simultaneous and non-simultaneous is ill-defined. Indeed, if the non-simultaneous associations occur non-preferentially with respect to the time of the TGF, as suggested by the distribution in Figure 1, then given the number of matches 5 ms either side of the TGF, one might expect from Poisson statistics that between one and three of the simultaneous matches are actually part of the lightning-related sample rather than due to the TGF. If the lightning-related events that are mis-classified as TGF emission are associated with longer TGFs, this further contributes to the match rate of longer TGFs being higher than expected from Relativistic Runaway Electron Avalanche (RREA) theory. Only 32 TGFs have non-simultaneous matches outside the window for simultaneity, and removing them from the sample of TGFs associated with WWLLN discharges tightens the anti-correlation between match rate and TGF duration, from which one can also conclude there is no correlation between the non-simultaneous match rate and TGF duration. These 32 associations from a total sample of 601 TGFs suggest a

detection efficiency of 5% for the IC lightning associated with TGFs. This is consistent with the estimates of *Abarca et al.* [2010] of 4.5% detection efficiency of WWLLN for IC lightning with peak currents greater than 15 kA. One TGF in our sample has both a simultaneous and a non-simultaneous association with WWLLN. The geolocations are 20 km apart, so a common origin is possible given the localization uncertainty of WWLLN [*Hutchins et al.*, 2012a]. If each TGF has both a simultaneous discharge and one associated with IC lightning that may not be simultaneous, then one might expect WWLLN to detect the IC lightning for the 154 TGFs it detected directly 5% of the time, giving seven or eight TGFs where both discharges are detected by WWLLN, yet we have only one such case. Two factors may explain this: each WWLLN station has a deadtime of ~ 1.3 ms following a detection, so that a smaller number of stations can detect the second discharge and the probability of detecting both discharges is reduced. The effect is probably more severe for the case where the TGF occurs first, given that the discharge with the higher-power TGF will incapacitate more stations than the lower-power IC discharge. The simultaneous and non-simultaneous discharges might also be mis-identified as duplicate measurements of the same discharge, a possibility that arises because it is common to make multiple measurements of a single discharge with different combinations of WWLLN stations and to remove the duplicate event manually. The factors leading the removal of duplicates are temporal coincidence (within 1 ms), common origin (20 km) and similar power. The power measurements can be subject to large uncertainties [*Hutchins et al.*, 2012b] so that a simultaneous or non-simultaneous event with an ill-constrained power measurement may have been mistakenly removed in this process, leading to a lower-than-expected number of cases where both the TGF and the IC lightning were detected. The

match rate for the non-simultaneous discharges is consistent with estimated efficiencies for WWLLN IC detection. Qualitatively the presence of one case where we detect both the non-simultaneous and simultaneous discharges is consistent with our hypothesis of 2 types of discharges for each TGF. The number of cases where both types of discharge are identified may be lower than expected because of network and processing inefficiencies for discharges this close in time and space.

The hypothesis that two different types of VLF signal are associated with TGFs is supported by differences in the characteristics of the radio signals of the two populations. Figure 4 shows that the median far-field radiated VLF stroke energy measured by WWLLN for the simultaneous discharges is much higher (3.1 kJ) than for the non-simultaneous discharges (700 J), with the latter typical of the median stroke energy for WWLLN [*Hutchins et al.*, 2012b]. In measurements of the wave-forms of radio discharges measured by the Duke telescopes in association with RHESSI-detected TGFs, *Lu et al.* [2011] find two types of pulses, with a slow ULF pulse accompanying the TGF (within the 2 ms timing uncertainty of RHESSI) and fast VLF pulses preceding the TGF. The ULF waveform may be the counterpart to the simultaneous WWLLN match and the fast VLF pulses akin to the non-simultaneous matches, but we note from Figure 1 that our non-simultaneous matches do not show a preferred order, whereas the fast VLF pulses of *Lu et al.* [2011] are all precursors to the TGF.

The identification of TGFs as the source of the radio emission in the simultaneous cases explains the tightness of the simultaneity ($\pm 40\,\mu$s) found by *Connaughton et al.* [2010] and suggested in prior studies using RHESSI data [*Inan et al.*, 1996; *Cummer et al.*, 2005; *Stanley et al.*, 2006; *Inan et al.*, 2006; *Lay*, 2008; *Cohen et al.*, 2006, 2010]. Our results

strongly suggest that two types of VLF radio signals are associated with TGFs: one, very strong and simultaneous with the TGF, is the TGF itself; the other, weaker and occurring up to several ms either side of the TGF, is a lightning event associated with the TGF.

Acknowledgments. The Fermi GBM Collaboration acknowledges support for GBM development, operations, and data analysis from National Aeronautics and Space Administration (NASA) in the United States and from the Bundesministerium für Wirtschaft und Technologie (BMWi) / Deutsches Zentrum für Luft und Raumfahrt (DLR) in Germany. This work was supported in part by NASA's Fermi Guest Investigator Program and by DARPA grant HR0011-10-1-0061. D.T. acknowledges support from Science Foundation Ireland under grant number 09-RFP-AST-2400. S.F. and G.F. acknowledge the support of the Irish Research Council for Science, Engineering and Technology; S.F. is cofunded by Marie Curie Actions under FP7. The authors wish to thank the World Wide Lightning Location Network (http://wwlln.net), a collaboration among over 50 universities and institutions, for providing the lightning location data used in this paper. We appreciate the freely-available Coyote resources for IDL programming, which helped generate all the histograms in this paper (http://www.idlcoyote.com/). We thank Nikolai Østgaard and an anonymous reviewer for helpful suggestions during the refereeing process.

References

Abarca, S. F., K. L. Corbosiero, and T. J. Galarneau, Jr (2010), An evaluation of the worldwide lightning location network (WWLLN) using the national lightning detection network (NLDN) as ground truth, *J. Geophys. Res.*, *115*, D18,206, doi: 10.1029/2009JD013411.

Briggs, M. S., G. J. Fishman, V. Connaughton, P. N. Bhat, W. S. Paciesas, R. D. Preece, C. Wilson-Hodge, V. L. Chaplin, R. M. Kippen, A. von Kienlin, C. A. Meegan, E. Bissaldi, J. R. Dwyer, D. M. Smith, R. H. Holzworth, J. E. Grove, and A. Chekhtman (2010), First results on terrestrial gamma-ray flashes from the Fermi gamma-ray burst monitor, *J. Geophys. Res.*, *115*, A07,323, doi:10.1029/2009JA015242.

Briggs, M. S., V. Connaughton, C. WilsonHodge, R. D. Preece, G. J. Fishman, R. M. Kippen, P. N. Bhat, W. S. Paciesas, V. L. Chaplin, C. A. Meegan, A. von Kienlin, J. Greiner, J. R. Dwyer, and D. M. Smith (2011), Electron-positron beams from terrestrial lightning observed with Fermi GBM, *Geophys. Res. Lett.*, *38*, L02,808, doi: 10.1029/2010GL046259.

Briggs, M. S., S. Xiong, V. Connaughton, D. Tierney, G. Fitzpatrick, S. Foley, E. Grove, A. Chekhtman, M. Gibby, G. J. Fishman, S. McBreen, V. L. Chaplin, S. Guiriec, E. Layden, P. N. Bhat, M. Hughes, J. Greiner, R. M. Kippen, C. A. Meegan, W. S. Paciesas, R. D. Preece, A. von Kienlin, C. Wilson-Hodge, R. H. Holzworth, , and M. L. Hutchins (2012), Terrestrial gamma-ray flashes in the fermi era: Improved observations and analysis methods, *J. Geophys. Res.*, *0*, 0.

Carlson, B. E., N. G. Lehtinen, and U. S. Inan (2010), Terrestrial gamma ray flash production by active lightning leader channels, *J. Geophys. Res.*, *115*, A10,324, doi: 10.1029/2010JA015647.

Celestin, S., and V. P. Pasko (2012), Compton scattering effects on the duration of terrestrial gamma-ray flashes, *Geophys. Res. Lett.*, *39*, L02,802, doi:10.1029/2011GL050342.

Cohen, M. B., U. S. Inan, and G. Fishman (2006), Terrestrial gamma ray flashes observed aboard the Compton gamma ray observatory/burst and transient source ex-

periment and ELV/VLF radio atmospherics, *J. Geophys. Res.*, *111*, D24,109, doi: 10.1029/2005JD006987.

Cohen, M. B., U. S. Inan, R. K. Said, and T. Gjestland (2010), Geolocation of terrestrial gamma-ray flash source lightning, *Geophys. Res. Lett.*, *37*, doi:10.1029/2009GL041753.

Collier, A. B., T. Gjesteland, and N. Østgaard (2011), Assessing the power law distribution of TGFs, *J. Geophys. Res.*, *116*, A10,320, doi:10.1029/2011JA016612.

Connaughton, V., M. S. Briggs, R. H. Holzworth, M. Hutchins, G. J. Fishman, C. A. Wilson-Hodge, V. L. Chaplin, P. N. Bhat, J. Greiner, A. von Kienlin, R. M. Kippen, C. A. Meegan, W. S. Paciesas, R. D. Preece, E. Cramer, J. R. Dwyer, , and D. M. Smith (2010), Associations between Fermi GBM terrestrial gamma-ray flashes and sferics from the WWLLN, *J. Geophys. Res.*, *115*, A12,307, doi:10.1029/2010JA015681.

Cummer, S. A., Y. Zhai, W. Hu, D. M. Smith, L. I. Lopez, and M. A. Stanley (2005), Measurements and implications of the relationship between lightning and terrestrial gamma ray flashes, *Geophys. Res. Lett.*, *32*, L08,811, doi:10.1029/2005GL022778.

Cummer, S. A., G. Lu, M. S. Briggs, V. Connaughton, S. Xion, G. J. Fishman, and J. R. Dwyer (2011), The lightning-tgf relationship on microsecond timescales, *Geophys. Res. Lett.*, *38*, L14,810, doi:10.1029/2011GL048099.

Dwyer, J. R. (2012), The relativistic feedback discharge model of terrestrial gamma ray flashes, *J. Geophys. Res.*, *117*, A02,308, doi:10.1029/2011JA017160.

Dwyer, J. R., and L. Babich (2011), Low-energy electron production by relativistic runaway electron avalanches in air, *J. Geophys. Res.*, *116*, A09,301, doi: 10.1029/2011JA016494.

Dwyer, J. R., and D. M. Smith (2005), A comparison between monte carlo simulations of runaway breakdown and terrestrial gamma-ray flash observations, *Geophys. Res. Lett.*, *32*, L22,804, doi:10.1029/2005GL023848.

Fishman, G. J., P. N. Bhat, R. Mallozzi, J. M. Horack, T. Koshut, C. Kouveliotou, G. N. Pendleton, C. A. Meegan, R. B. Wilson, W. S. Paciesas, S. J. Goodman, and H. J. Christian (1994), Discovery of intense gamma-ray flashes of atmospheric origin, *Science*, *264*, 1313–1316.

Fishman, G. J., M. S. Briggs, V. Connaughton, P. N. Bhat, W. S. Paciesas, A. von Kienlin, C. Wilson-Hodge, R. M. Kippen, R. Preece, C. A. Meegan, and J. Greiner (2011), Temporal properties of terrestrial gamma-ray flashes from the gamma-ray burst monitor on the Fermi observatory, *J. Geophys. Res.*, *116*, A07,304, doi:10.1029/2010JA016084.

Fuschino, F., F. Longo, M. Marisald, et al. (2009), AGILE view of TGFs, in *Conf. Proc. 1118, Coupling of Thunderstorms and Lightning Discharges to Near-Earth Space*, edited by N. B. Crosby, T.-Y. Huang, and M. J. Rycroft, pp. 46–51, AIP.

Gjesteland, T., N. Østgaard, P. H. Connell, J. Stadsnes, and G. J. Fishman (2010), Effects of dead time losses on terrestrial gamma ray flash measurements with the Burst and Transient Source Experiment, *J. Geophys. Res.*, *115*, A00E21, doi: 10.1029/2009JA014578.

Gjesteland, T., N. Østgaard, A. B. Collier, B. E. Carlson, M. B. Cohen, and N. G. Lehtinen (2011), Confining the angular distribution of terrestrial gamma ray flash emission, *J. Geophys. Res.*, *116*, A11,313, doi:10.1029/2011JA016716.

Gjesteland, T., N. Østgaard, A. B. Collier, B. E. Carlson1, C. Eyles, and D. M. Smith (2012), A new method reveals more TGFs in the RHESSI data, *Geophys. Res. Lett.*,

doi:10.1029/2012GL050899.

Grefenstette, B. W., D. M. Smith, J. R. Dwyer, and G. J. Fishman (2008), Time evolution of terrestrial gamma ray flashes, *Geophys. Res. Lett.*, *35*, L06,802, doi: 10.1029/2007GL032922.

Grefenstette, B. W., D. M. Smith, B. J. Hazelton, and L. I. Lopez (2009), First RHESSI terrestrial gamma ray flash catalog, *J. Geophys. Res.*, *114*, A02,314, doi: 10.1029/2008JA013721.

Hazelton, B. J., B. W. Grefenstette, D. M. Smith, J. R. Dwyer, X.-M. Shao, S. A. Cummer, T. Chronis, E. H. Lay, and R. H. Holzworth (2009), Spectral dependence of terrestrial gamma-ray flashes on source distance, *Geophys. Res. Lett.*, *36*, L01,108, doi:10.1029/2008GL035906.

Hutchins, M. L., R. H. Holzworth, J. B. Brundell, and C. J. Rodger (2012a), Relative detection efficiency of the world wide lightning location network, *Radio Sci*, *0*, 0.

Hutchins, M. L., R. H. Holzworth, C. J. Rodger, and J. B. Brundell (2012b), Far-field power of lightning strokes as measured by the world wide lightning location network, *J. Atmos. Oceanic Technol.*, *29*, 1102–1110.

Inan, U. S., S. C. Reising, G. J. Fishman, and J. M. Horack (1996), On the association of terrestrial gamma-ray bursts with lightning and implications for sprites, *Geophys. Res. Lett.*, *23*, 1017–1020.

Inan, U. S., M. B. Cohen, R. K. Said, D. M. Smith, and L. I. Lopez (2006), Terrestrial gamma ray flashes and lightning discharges, *Geophys. Res. Lett.*, *33*, L18,802, doi: 10.1029/2006GL027085.

Jacobson, A. R., R. Holzworth, J. Harlin, R. Dowden, and E. Lay (2006), Performance assessment of the world wide lightning location network (wwlln), using the los alamos sferic array (lasa) array as ground-truth, *J. Atmos. Oceanic Technol.*, *23*, 1082–92.

Lay, E. H. (2008), Investigating lightning-to-ionosphere energy coupling based on VLF lightning propagation characterization, Ph.D. thesis, University of Washington.

Liu, N., and V. P. Pasko (2004), Effects of photoionization on propagation and branching of positive and negative streamers in sprites, *J. Geophys. Res.*, *109*, A04,301, doi: 10.1029/2003JA010064.

Lu, G., R. J. Blakeslee, J. Li, D. M. Smith, X.-M. Shao, E. W. McCaul, D. E. Buechler, H. J. Christian, J. M. Hall, and S. A. Cummer (2010), Lightning mapping observation of a terrestrial gammaray flash, *Geophys. Res. Lett.*, *37*, L11,806, doi:10.1029/2010GL043494.

Lu, G., S. A. Cummer, J. Li, F. Han, D. M. Smith, and B. W. Grefenstette (2011), Characteristics of broadband lightning emissions associated with terrestrial gamma ray flashes, *J. Geophys. Res.*, *116*, A03,316, doi:10.1029/2010JA016141.

Marisaldi, M., F. Fuschino, C. Labanti, M. Galli, F. Long, E. D. Monte, et al. (2010a), Detection of terrestrial gamma-ray flashes up to 40 MeV by the AGILE satellite, *J. Geophys. Res.*, *115*, A00E13, doi:10.1029/2009JA014502.

Marisaldi, M., A. Argan, A. Trois, A. Giuliani, M. Tavani, C. Labanti, F. Fuschino, et al. (2010b), Gamma-ray localization of terrestrial gamma-ray flashes, *Phys. Rev. Lett*, *105*, 128,501, doi:10.1103/PhysRevLett.105.128501.

Morrow, R., and J. J. Lowke (1997), Streamer propagation in air, *J. Phys. D: Appl. Phys.*, *30*, 614–627.

Østgaard, N., T. Gjesteland, J. Stadsnes, P. H. Connell, and B. Carlson (2008), Production altitude and time delays of the terrestial gamma flashes: Revisiting the burst and transient source experiment spectra, *Journal of Geophys. Res.*, *113*, A02,307, doi: 10.1029/2007JA012618.

Rodger, C. J., J. B. Brundell, R. H. Holzworth, and E. H. Lay (2009), Growing detection efficiency of the world wide lightning location network, in *Conf. Proc. 1118, Coupling of Thunderstorms and Lightning Discharges to Near-Earth Space*, edited by N. B. Crosby, T.-Y. Huang, and M. J. Rycroft, pp. 15–20, AIP.

Smith, D. M., L. I. Lopez, R. P. Lin, and C. P. Barrington-Leigh (2005), Terrestrial gamma-ray flashes observed up to 20 MeV, *Science*, *307*, 1085–1088.

Stanley, M. A., X.-M. Shao, D. M. Smith, L. I. Lopez, M. B. Pongratz, J. D. Harlin, M. Stock, and A. Regan (2006), A link between terrestrial gamma-ray flashes and intracloud lightning discharges, *Geophys. Res. Lett.*, *33*, L06,803, doi: 10.1029/2005GL025537.

Uman, M. A. (2001), *The Lightning Discharge*, Dover, 1249 Mineola, New York.

Figure 1. The top panel shows the offset distribution, in 500 μs bins, of the TGF peak - the mid-point of the T_{50} interval (see text) - from 186 matched discharge times of group arrival measured by WWLLN. The lower plot zooms in on the region close to the TGF peak, containing most of the GBM-WWLLN matches. A 400 μs interval centered on the TGF peak is used to define GBM-WWLLN simultaneity, and contains 154 of the associations.

Figure 2. The top panel shows the duration distribution in 50 μs time bins of the 594 TGFs (salmon) with the subset of 154 TGFs having a match with a simultaneous WWLLN discharge shown in blue. We exclude likely electron-beam TGFs, which are generally much longer than the TGFs detected in gamma rays [*Briggs et al.*, 2011], and suppress for display purposes the two likely gamma-ray TGFs that have durations longer than 1 ms. In the bottom panel we rebin the distributions such that each time bin contains at least ten TGFs with associated simultaneous WWLLN discharges (the final, large, bin has no matches in the WWLLN data). The asterisks show the fraction of TGFs having WWLLN associations.

Figure 3. The top panel shows the duration distribution in 50 μs time bins of the 594 TGFs (salmon) with the subset of 154 TGFs having a match with a simultaneous WWLLN discharge shown in blue. In the bottom panel we rebin the distributions such that each time bin contains at least ten TGFs with associated simultaneous WWLLN discharges. The asterisks show the fraction of TGFs having WWLLN associations. Similar to Figure 2 but with the T_{50}s measured for counts detected above 300 keV. Compared to Figure 2, the width of the T_{50} values is narrower and peaked at lower values for those TGFs with WWLLN associations. The number of very short TGFs with associations is also higher, and the number of longer TGFs with associations lower than when the T_{50} values are measured using the entire GBM energy range.

Figure 4. The estimated far-field VLF stroke energy of discharges measured by WWLLN in association with GBM-detected TGFs. *Hutchins et al.* [2012a] describe the procedure and reliability of measuring energies associated with WWLLN discharges. We include here 164 WWLLN discharges associated with TGFs for which energy measurements are available, and which have uncertainties lower than 70% of their value. The subset of non-simultaneous associations, which are farther than $\pm$200 μs from the TGF peak, is shown in blue, the simultaneous associations in salmon. The non-simultaneous discharges have a significantly lower median energy (700 J) than the simultaneous discharges (3.1 kJ).

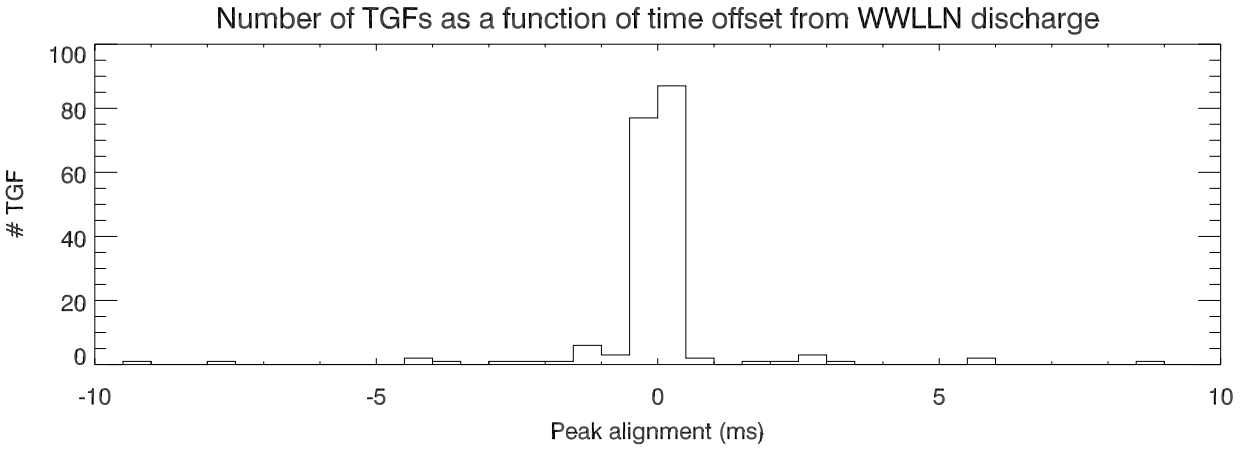
Number of TGFs as a function of time offset from WWLLN discharge
TGF
100
80
60
40
20
0
-10
-5
0
5
10
Peak alignment (ms)

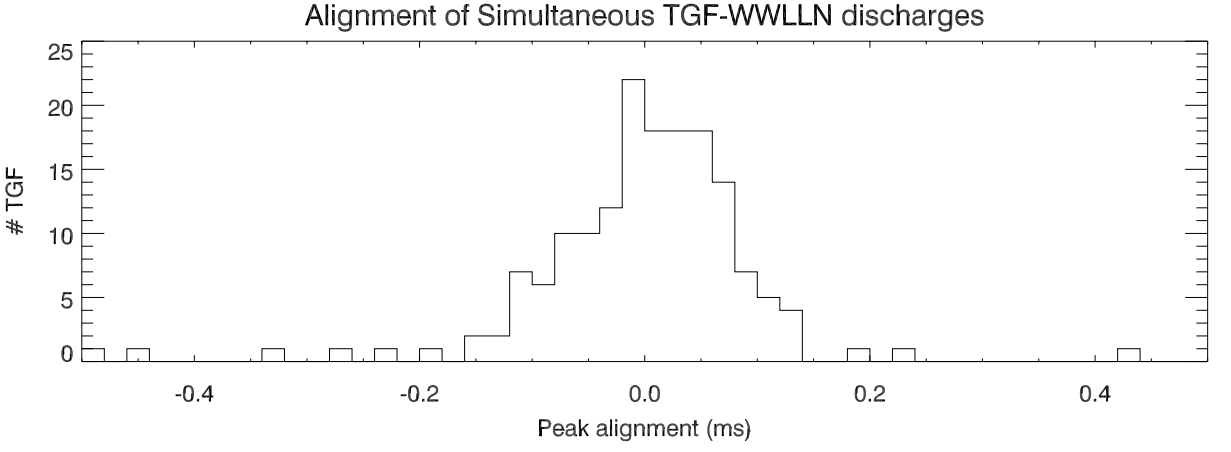
Alignment of Simultaneous TGF-WWLLN discharges
TGF
25
20
15
10
5
0
-0.4
-0.2
0.0
0.2
0.4
Peak alignment (ms)

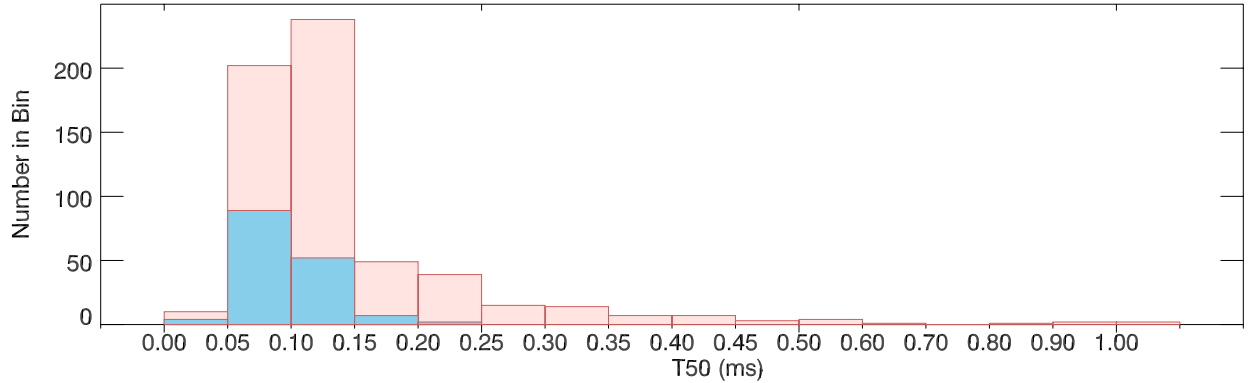
Number in Bin
200
150
100
50
0
0.00
0.05
0.10
0.15
0.20
0.25
0.30
0.35
0.40
0.45
0.50
0.60
0.70
0.80
0.90
1.00
T50 (ms)

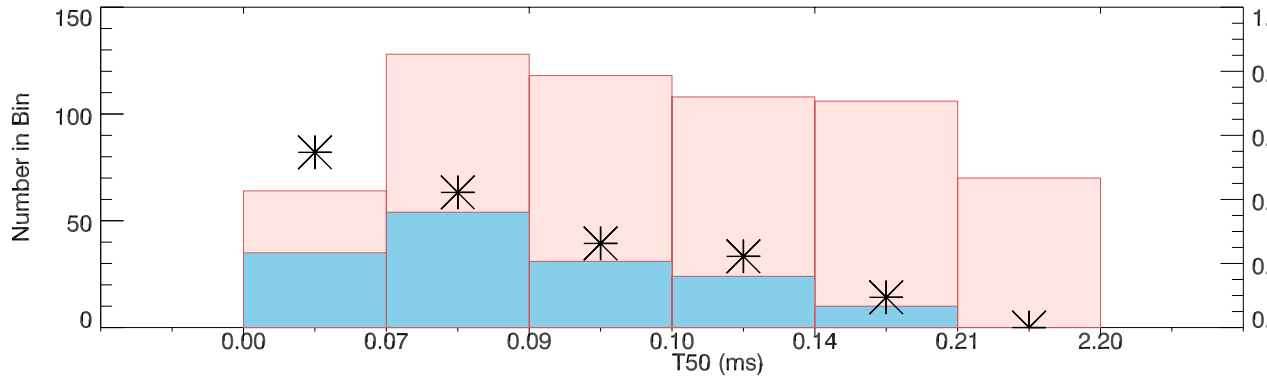
Number in Bin
150
100
50
0
0.00
0.07
0.09
0.10
0.14
0.21
2.20
T50 (ms)
Fraction of WWLLN matches
1.0
0.8
0.6
0.4
0.2
0.0

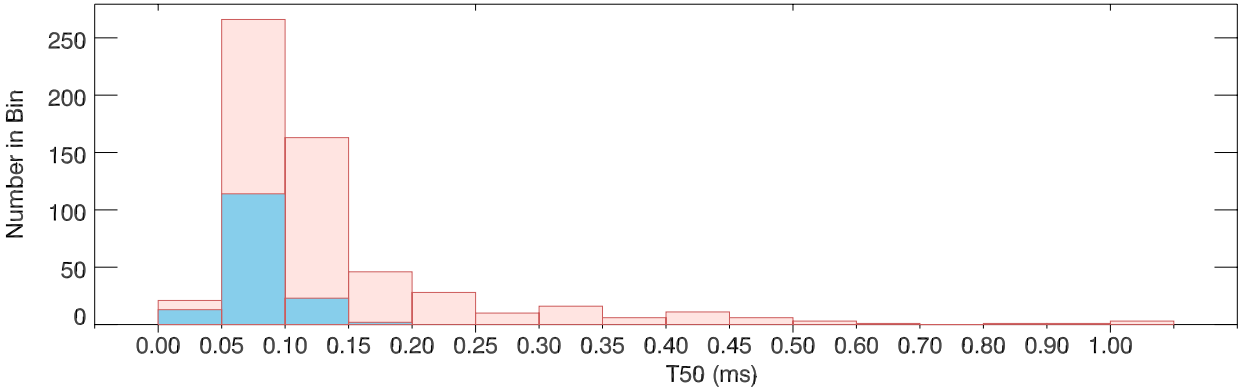
Number in Bin
250
200
150
100
50
0
0.00 0.05 0.10 0.15 0.20 0.25 0.30 0.35 0.40 0.45 0.50 0.60 0.70 0.80 0.90 1.00
T50 (ms)

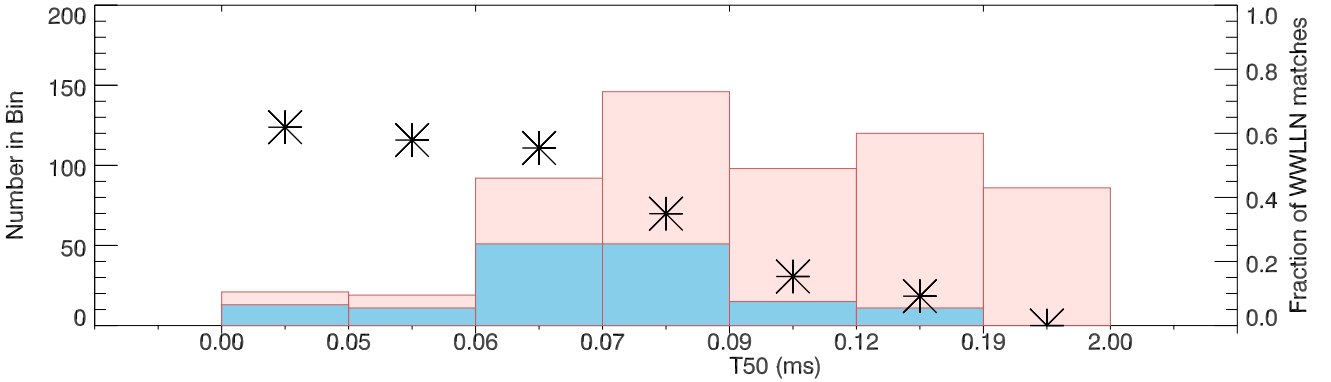
Number in Bin
200
150
100
50
0
0.00 0.05 0.06 0.07 0.09 0.12 0.19 2.00
T50 (ms)
Fraction of WWLLN matches
1.0
0.8
0.6
0.4
0.2
0.0

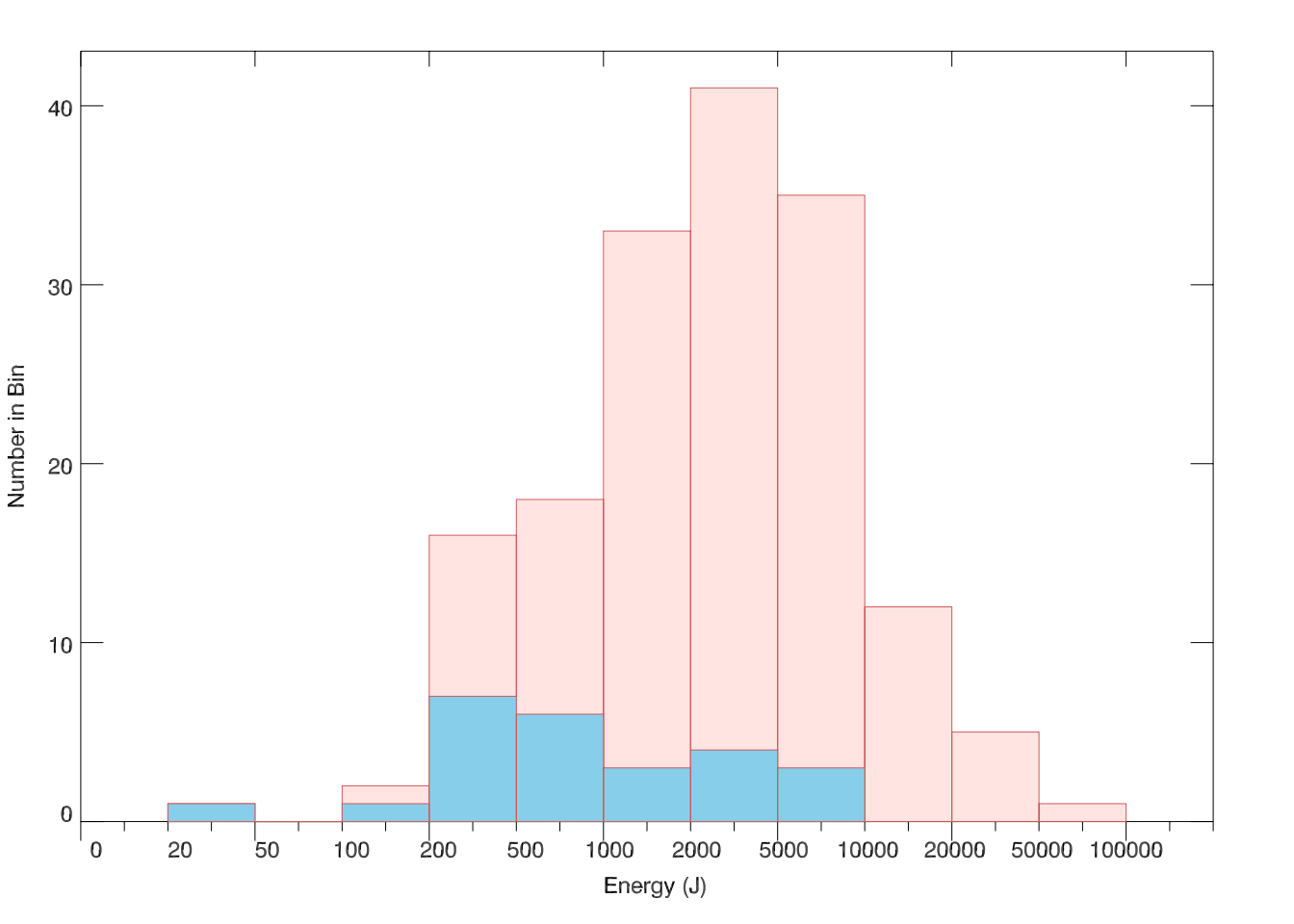
Number in Bin
0
10
20
30
40
0
20
50
100
200
500
1000
2000
5000
10000
20000
50000
100000
Energy (J)